

OSMDA: OpenStreetMap-based Domain Adaptation for Remote Sensing VLMs

Stefan Maria Ailuro, Mario Markov, Mohammad Mahdi, Delyan Boychev,
Luc Van Gool, and Danda Pani Paudel

INSAIT, Sofia University “St. Kliment Ohridski”

stefan.ailuro@insait.ai

arXiv:2603.11804v1 [cs.CV] 12 Mar 2026

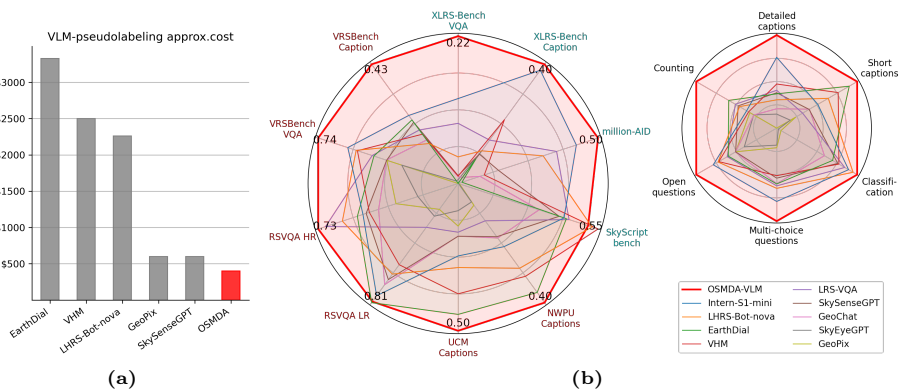


Fig. 1: (a) Estimated data generation costs based on API pricing and measured self-hosting costs. (b) Performance per benchmark and task-aggregated performance. Benchmarks used at fine-tuning are highlighted in purple color, zero-shot benchmarks highlighted in teal color.

Abstract. Vision–Language Models (VLMs) adapted to remote sensing rely heavily on domain-specific image–text supervision, yet high-quality annotations for satellite and aerial imagery remain scarce and expensive to produce. Prevailing pseudo-labeling pipelines address this gap by distilling knowledge from large frontier models, but this dependence on large teachers is costly, limits scalability, and caps achievable performance at the ceiling of the teacher. We propose OSMDA: a self-contained domain adaptation framework that eliminates this dependency. Our key insight is that a capable base VLM can serve as its own annotation engine: by pairing aerial images with rendered OpenStreetMap (OSM) tiles, we leverage optical character recognition and chart comprehension capabilities of the model to generate captions enriched by OSM’s vast auxiliary metadata. The model is then fine-tuned on the resulting corpus with satellite imagery alone, yielding OSMDA-VLM, a domain-adapted VLM that requires no manual labeling and no stronger external model. We

conduct exhaustive evaluations spanning 10 benchmarks across image-text-to-text tasks and comparing against 9 competitive baselines. When equally mixed with real data, our method achieves state-of-the-art results, while being substantially cheaper to train than teacher-dependent alternatives. These results suggest that, given a strong foundation model, alignment with crowd-sourced geographic data is a practical and scalable path towards remote sensing domain adaptation. Dataset and model weights will be made publicly available.

Keywords: Remote Sensing · Vision-Language Models · Domain Adaptation

1 Introduction

The success of large vision-language models (VLMs) across a broad range of perception and reasoning tasks has naturally prompted their application to remote sensing, a domain characterised by an abundance of satellite and aerial imagery but a persistent shortage of structured, task-specific annotations. Early attempts at adapting general-purpose VLMs to this domain have relied on small curated datasets and rule-based data augmentation [15], yielding only modest performance improvements. A more productive line of work has turned to pseudo-labeling: large, annotation-rich corpora are synthesized by pairing remote sensing images with text generated either through rule-based repurposing of scarce human-annotated datasets [18, 62, 63] or, increasingly, by prompting powerful closed-source models such as GPT-4V [36] or Gemini-Vision [47]. The resulting labeled datasets have driven measurable progress, and several specialized remote sensing VLMs have emerged from this paradigm [24, 39, 40].

Yet the dominant strategy carries a fundamental tension. Querying frontier general-purpose models at scale is expensive, increasingly so as dataset sizes grow. More critically, distilling a weaker student from a stronger teacher imposes a hard ceiling on what the student can learn: the student cannot surpass the teacher’s own understanding of the domain, and any errors or hallucinations in the teacher’s output are faithfully absorbed. As foundation models improve rapidly, any particular distillation pipeline is liable to be overtaken not by better engineering but simply by upgrading the base model, suggesting that elaborate data synthesis machinery may offer diminishing returns compared to efforts on increasing the expert-annotated data corpus or judicious selection of the base model itself. For instance, the general-purpose Intern-S1 [3] model achieves SOTA performance on XLRs-Bench [52], outperforming specialized models in extremely-high-resolution satellite tasks.

This observation motivates a different perspective: rather than investing resources in increasingly sophisticated pseudolabel generation, we propose to prioritize cheap, scalable alignment methods that can be applied to whichever frontier model is available. The question then becomes whether a high-quality base model, paired with noisy but freely available geographic supervision, is suffi-

cient to achieve competitive domain adaptation without any recourse to external teachers.

Our experiments suggest so, and we propose the **OSMDA** method: OSM-based Domain Adaptation. Rich domain information is scoured from OpenStreetMap [38], a global crowd-sourced geographic database, covering much of the Earth’s surface: road networks, land-use polygons, points of interest, functional usage, and more. We render this data as raster map tiles in OSM-carto [2] style, geographically co-registered with satellite images, by utilizing the Mapnik [41] library – a format meticulously constructed by geography experts for human perception. When the base VLM is presented with such a map alongside the satellite image, it can read and place names, road labels, and land-cover categories directly from the map image, and reason about their spatial arrangement and functionality to construct a detailed caption of the area. Our method exploits capabilities already present in modern VLMs (optical character recognition and chart comprehension) to bootstrap its own geographic supervision. Thus, the same model can be used as an annotator, and later as a student model trained to infer the OSM-derived information from RGB satellite images alone. The entire pipeline is self-contained: it requires no API access, no proprietary data, and no expert-level human labels beyond what OpenStreetMap volunteers have contributed. Employing the OSMDA method, we introduce **OSMDA-Captions**: a dataset grounded in verifiable geographic structures, without any human annotator or external model in the loop. Combining it with various external remote sensing datasets, we produce **OSMDA-VLM**: a domain-adapted model achieving state-of-the-art performance on remote sensing tasks.

We evaluate OSMDA-VLM on 10 benchmarks of varied difficulty spanning captioning, counting, multiple-choice, and open-ended visual question answering (VQA), and classification. Because we observe that many published baselines are brittle to instruction format, failing under paraphrases or zero-shot conditions, we evaluate all nine competitors under unified evaluation protocols. We believe this evaluation constitutes one of the most thorough comparative studies in remote sensing VLM literature.

We summarise our contributions as follows:

- **OSMDA**: a self-contained domain adaptation framework that uses map comprehension to generate geographic supervision for VLM fine-tuning, eliminating dependence on external teacher models and significantly reducing annotation cost (see Figure 1(a)).
- **OSMDA-Captions**: a high-quality dataset of over 200K detailed image-caption pairs incorporating OpenStreetMap data.
- **OSMDA-VLM**: a remote sensing VLM achieving state-of-the-art results across the majority of evaluated remote sensing benchmarks (see Figure 1(b)).
- A comprehensive and reproducible evaluation of ten models under unified protocols across ten benchmarks, exposing systematic overfitting in prior work and providing a more reliable assessment of the current state of the field.

Table 1: (a) Remote Sensing VLMs: student model architecture, teacher model used for pseudo-labelling, number of generated samples $N_{gen.}$, and approximate cost $C_{appr.}$ of generation based on teachers’ API cost or measured self-hosting cost. Methods further differ by architectural modifications and varying sources of weak annotations. N_{evals} states the total number of evaluations and reevaluations of RS-VLMs in the image-text-to-text setting conducted in each model’s corresponding work.

Method	Student model	Teacher model	$N_{gen.}$	$C_{appr.}$	N_{evals}
LRS-VQA [32]	LLaVA-Next-7B	rule-based	-	-	6
SkyEyeGPT [62]	MiniGPT-v2-7B	rule-based	-	-	5
GeoChat [18]	LLaVA-1.5-7B	Vicuna-v1.5	320k	\$200	5
GeoPix [39]	LLaVA-1.5-7B	GPT-4o	140k	\$600	6
SkySenseGPT [31]	LLaVA-1.5-7B	GPT3.5 & GPT4	180k	\$600	10
VHM [40]	LLaVA-1.5-7B	Gemini-Vision	1.4M	\$2500	8
LHRS-Bot-nova [24]	SigLip + Llama3-8B	ShareCaptioner & GPT-4v	1.4M	\$2260	11
EarthDial [45]	InternViT + Phi-3-4B	InternLM-XComposer2	11.8M	\$3330	16
OSMDA-VLM	InternVL3.5-8B	InternVL3.5-8B	200k	\$400	100

2 Related Works

Vision-Language Models. Modern VLMs are built around a shared architecture: a visual encoder (typically a ViT [8] pretrained with contrastive objectives such as CLIP [43]) produces patch-level embeddings, a lightweight connector (usually MLP projector or Q-Former [20]) maps these into the token space of a large language model, and the LLM generates free-form text conditioned on both visual and language tokens. Systems such as LLaVA [25], InstructBLIP [6], and MiniGPT-4 [65] demonstrated that instruction-tuning this architecture on relatively modest volumes of curated multimodal data produces models that generalize well across diverse vision-language tasks. Subsequent work has scaled the visual encoder, diversified the connector design, improved high-resolution handling through dynamic tiling strategies, and expanded training data to billions of image–text pairs. InternVL [54], the model family we build on, exemplifies this progression: it uses a large ViT trained jointly with an LLM via a progressive alignment procedure and achieves competitive performance across open benchmarks. A key empirical observation underpinning our work is that the quality of the pretrained backbone is the primary driver of downstream performance, with fine-tuning data playing a secondary, corrective role.

Domain adaptation and instruction tuning. Adapting a general-purpose VLM to a new domain usually follows a major paradigm: continued pretraining on domain-specific image-text pairs updates the visual-language alignment before any task-specific supervision is introduced; instruction tuning then teaches the model to follow diverse query formats using curated question-answer datasets [19, 25, 65]. When labeled domain data is scarce – the typical situation in remote sensing – these stages rely on either manual annotation or automatically

generated pseudo-labels [11, 17]. Pseudo-labeling with frozen, stronger models (self-training, knowledge distillation) has become a dominant strategy in both NLP and vision [34, 53], though it inherits the teacher’s errors and imposes an asymptotic ceiling on student performance.

VLMs in remote sensing. The adaptation of VLMs to remote sensing has accelerated substantially since 2023. RSGPT [15] was among the first to fine-tune a general VLM on a small, human-annotated RS captioning corpus, establishing a baseline for the field. GeoChat [18] extended this to a grounded, multitask setting, introducing the first RS VLM capable of region-level dialogue and visually grounded responses. SkyEyeGPT [62] and SkySenseGPT [31] followed with larger instruction-tuning datasets and improved handling of fine-grained spatial relations. LHRS-Bot [35] and its successor LHRS-Bot-Nova [24] emphasised pretraining at scale – first on a four-million-pair image-text corpus – before instruction tuning, proposing an enhanced vision encoder and bridge layer for better language-vision alignment. VHM [40] focused on breadth and truthfulness, constructing a rich-caption dataset and an honest instruction set that includes deceptive questions to prevent the model from hallucinating affirmative answers. EarthDial [45] scaled further still, covering multi-spectral, multi-temporal, and multi-resolution imagery with over 11 million instruction pairs. GeoPix [39] extended the paradigm to pixel-level understanding, coupling image- and region-level dialogue with referring segmentation via a class-wise learnable memory module. Recent advancements moved on to enhance these models with reasoning and research on applications [21, 22, 26, 33, 51, 58], however these still rely on base RS-VLMs, which, while demonstrating steady progress driven primarily by data scaling and architectural refinements, still share a common dependency: high-quality supervision is ultimately sourced from either costly large general-purpose models or powerful proprietary models. We provide a comparison of preceding works in Table 1.

Pseudo-labeling pipelines. The practical challenge of constructing large RS instruction datasets has driven a broad range of automated labeling strategies, with an observable trend toward increasingly powerful external models. GeoChat [18] generated its 318k-sample instruction corpus by prompting Vicuna to reformat existing task-specific RS datasets into VQA and captioning templates – an early, cheap approach that keeps the teacher lightweight but limits semantic richness and visual grounding. SkyEyeGPT’s SkyEye-968k dataset [62] took an even more conservative stance, relying primarily on rule-based conversation templates derived from public RS annotations, with model-generated content kept minimal to control quality. GeoPix built its GeoPixInstruct dataset [39] from detection corpora and deployed GPT-4o [37] with few-shot spatial arrangement examples to generate instance-level descriptions, further refining a subset through human-in-the-loop GPT-4o [37] fine-tuning. SkySenseGPT [31] escalated both scale and teacher strength: its FIT-RS corpus of 1.8 million samples is built on the manually annotated STAR scene-graph dataset, with TinyLLaVA [64],

GPT-3.5, and GPT-4 [36] applied for initial image detailed captioning, while relation-reasoning instructions are generated in a rule-based manner. VHM [40] followed a similar escalation, generating its VersaD pretraining corpus of 1.4 million images via few-shot Gemini Vision [47] prompting, explicitly instructing the model to include metadata, object attributes, and scene context that simpler pipelines omit, then using language-only Gemini to construct VersaD-Instruct fine-tuning dataset. LHRS-Bot-Nova [24] used Share-Captioner [4] for its LHRS-Align-Recap pretraining dataset over 1.1 million images, paired with their OpenStreetMap features, and GPT-4V [36] for its LHRS-Instruct-Plus instruction tuning dataset. EarthDial [45] pushed scale to its current extreme, generating over 11 million instruction pairs spanning multiple modalities, using InternLM-XComposer2 [7] for captioning across a mix of real RS datasets and OSM-aligned imagery.

OpenStreetMap [38] has also been used as a supervision source for million-scale image-text datasets. SkyScript [55] geo-aligned OSM tags with satellite images, filtered these by CLIP-similarity to acquire a set of 1.5 million objects, then used GPT to convert raw key-value tag sets into short natural language descriptions. ChatEarthNet [60] took an analogous approach at the Sentinel-2 [9] scale, grounding captions in ESA WorldCover [61] land-cover labels and generating richer descriptions for 173k image patches via GPT-3.5 and GPT-4V [36]. RSTeller [12] proposed a similar workflow over 1.3 million NAIP [10] images, extracting OSM feature tags for each tile and passing them to an LLM to produce two dense captions per image; despite its scale, coverage is limited to the continental United States and the NAIP resolution range, restricting geographic generalizability. All three of these datasets share the same fundamental pipeline: OSM data is parsed into discrete key-value tags and simplified geometries, which are then converted to text by Mixtral-Nemo [16] and filtered by human and GPT-4. The map itself is never seen by the model; topography, layout, and objects’ adjacency are discarded at the tag-extraction stage.

Our approach incorporates both semantic and geometric information. Rather than just parsing OSM into tags, we render it as a map tile in OSM-carto style and present both the satellite image and map to the base VLM simultaneously. The model reads place names, road labels, land-cover polygons, and their spatial arrangement directly from the rendered image using its OCR capability, and generates captions and QA pairs grounded in that visual geographic context. This preserves topographical information that tag-based pipelines discard, and, crucially, requires no external model stronger than the base VLM itself.

3 Method. OSM-based domain adaptation

Our pipeline consists of three stages: (1) data curation – selecting a high-quality, geographically diverse subset of satellite images paired with OSM annotations; (2) map rendering – converting raw OSM data into semantically rich, VLM-readable map tiles co-registered with each image; and (3) caption generation – prompting the base VLM with paired satellite image and rendered map to

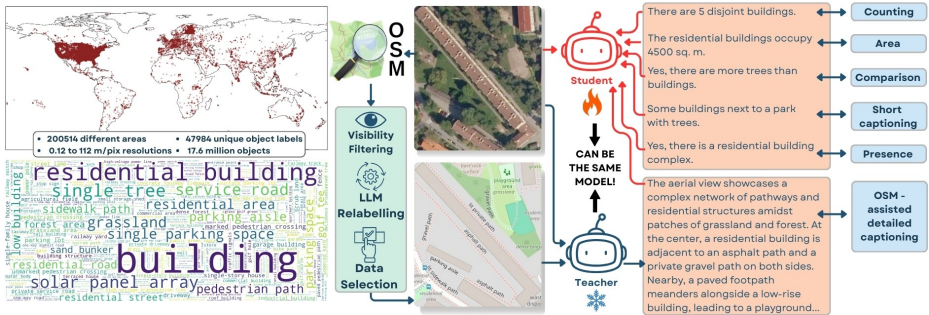


Fig. 2: The creation of OSMDA-Captions and OSMDA-VLM via the OSMDA method. We collect images of various areas and resolutions, and fetch their OSM object tags. We filter out visible objects using the image resolution and a set of heuristics, then send each object’s OSM tags through an LLM to produce a short label capturing its essence. We overlay the labels onto OSM map tiles and feed the resulting overlays, alongside the matching satellite images, to the base VLM to generate OSMDA-Captions – a detailed captioning dataset incorporating OSM metadata. We then mix this dataset with existing remote-sensing data and fine-tune the base model, producing OSMDA-VLM - a state-of-the-art model specializing in the remote-sensing domain.

produce the OSMDA-Captions training corpus. Fine-tuning then proceeds on satellite images alone, making the final model map-free at inference time. An overview of the pipeline is shown in Figure 2.

3.1 Image and OSM Data Curation

We use the training split of SkyScript [55] as the source of our base imagery, specifically its 30% CLIP-score-filtered subset containing approximately 1.5 million georeferenced satellite images. Each image is associated with a geographic bounding box footprint, which allows us to retrieve the corresponding OSM objects through spatial queries.

OSM object filtering. Raw OSM data contains a large proportion of objects that are either not visually grounded or semantically irrelevant for image understanding. We apply a visibility heuristic to remove objects that cannot be observed from above: underground infrastructure, administrative and legal boundaries, and similar non-visible features are discarded. In a separate pass, we strip all tags that carry identifying or commercially sensitive information – postal addresses, place names, phone numbers, business names, operators, opening hours, and ownership metadata – to anonymize the data and prevent the model from learning to hallucinate specific named entities from visual context. After filtering, the remaining pool contains approximately 4.5 million unique object descriptions, each described by its retained functional OSM tags.

Semantic labelling. The filtered tag sets are concise but numerous and not naturally readable as object labels: a tag like `amenity=fuel; canopy=yes` is technically correct but linguistically impoverished. We process each unique set of object tags with Qwen2.5-72B-Instruct [59], instructing it to produce a brief (2–3 word) descriptive label that captures the object’s visual and functional identity. The total cost of this labelling step is negligible at this scale. The resulting vocabulary spans 48k unique semantic labels, substantially richer than the 29k labels produced by SkyScript’s rule-based heuristics.

Distribution balancing. The distribution of object occurrences across images is highly skewed: common categories such as buildings, roads, and parks dominate the dataset, while semantically informative but rarer classes such as helipads, weirs, and salt marshes appear in only a small number of images. Training directly on this raw distribution would bias the model toward frequent scene types and limit its ability to learn minority geographic concepts.

To mitigate this issue, we apply a data-centric balancing procedure inspired by the Meta-CLIP probabilistic curation framework [57]. Images are treated as queries and assigned sampling weights based on the inverse frequency of their associated semantic labels, as well as the total number of objects present in each image. A balanced subset is then sampled according to these weights.

To further improve diversity and remove redundancy, we compute DINOv3 [44] visual feature embeddings for all images and perform K-means clustering in this embedding space. This allows us to identify visually similar samples and select representative images from each cluster, effectively removing near-duplicates while preserving dataset diversity. The resulting curated dataset contains 200514 high-quality satellite images paired with their corresponding OSM object annotations, with substantially improved balance across semantic categories.

3.2 Map Rendering

For each curated image, we render a raster map tile co-registered to its pixel extent using Mapnik [41] with the `openstreetmap-carto` stylesheet [2]. OSM objects are first classified into semantic layer groups (landuse, natural, water, roads, buildings, amenities...) and filtered by zoom level to suppress objects whose geometry falls below the resolution-appropriate visibility threshold. Polygon and area features are rendered with fill textures and colors drawn from the `carto` style that visually encode land-use and land-cover semantics – residential areas, farmland, forest, and water each receive a distinct visual treatment. Linear features (roads, railways, waterways) are stroked with widths and styles reflecting their functional class. Point features (transport nodes, amenities, utilities) are rendered as symbolic icons from the `carto` icon set.

For text labels, we substitute the default `openstreetmap-carto` label sources – toponym names, address lines, amenity labels, place names – with the 2–3 word semantic labels generated in Section 3.1. Mapnik’s label placement engine handles priority ordering and overlap resolution automatically, placing higher-priority labels (arterial roads, large landuse polygons) before lower-priority ones

and suppressing labels that would occlude higher-ranked neighbours. The output is a map tile that is visually structured like a standard OSM rendering but carries our cleaned, anonymised, semantically standardised vocabulary in place of free-text toponyms. This design makes the rendered map simultaneously information-dense and legible to the VLM’s OCR pathway, without exposing the model to personally identifying or commercially biasing text.

3.3 Pseudo-labelling. OSMDA-Captions corpus

The teacher model generates the caption corpus. Each sample is presented as a two-image prompt: the satellite image followed by its co-registered rendered map. The model is instructed to produce a detailed geographic caption that integrates visual evidence from the aerial image with the semantic structure readable from the map. It is prompted to use a confident, declarative tone, to avoid speculations and guesses, not to mention the map and labeling system in any way (the full prompt is provided in the supplementary). Crucially, generation is stochastic with temperature $T = 1.0$, this ensures that semantically equivalent scenes receive linguistically varied captions across the corpus, preventing the fine-tuning stage from mode collapse. We refer to the resulting 200k caption dataset as OSMDA-Captions. At fine-tuning time, only the satellite image is provided as input; the rendered map is not used. The model must therefore learn to produce geographically grounded descriptions from visual features alone.

3.4 Domain adapted VLM

To fully prepare and adapt the VLM to remote sensing domain, a joint mixture of OSMDA-Captions and real labelled data from the training splits of the downstream benchmarks is used. The two sources are mixed at equal weight as a trade-off: OSMDA-Captions provide broad geographic coverage and semantically rich supervision derived from OSM structure, while the real benchmark data re-anchors the model to the downstream tasks and output formats expected at evaluation time. Details are provided in Section 4. Training on either source alone is suboptimal – OSM-derived captions alone may shift the model away from benchmark-specific conventions, while benchmark data alone is too sparse and narrow to inject substantive geographic knowledge. Joint training mitigates potential shifts or collapses and allows the model to simultaneously absorb the geographic grounding encoded in the synthetic captions and align to the downstream task distribution, with neither objective dominating the other.

4 Experiments

4.1 OSM-based domain adaptation

Benchmarks, metrics, and baselines. We benchmark on a total of ten datasets: five which contain separate training splits for fine-tuning - NWPU-

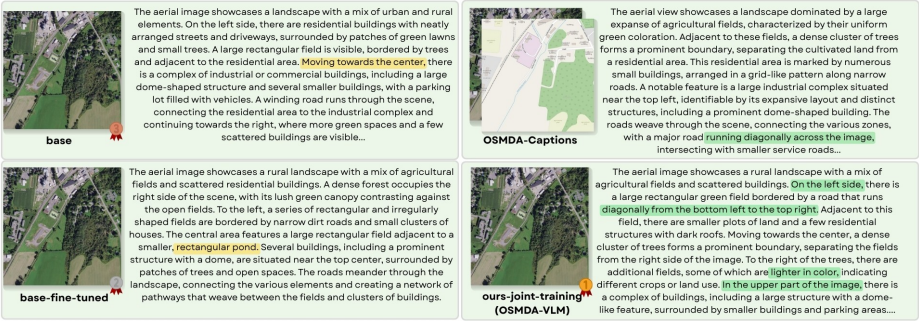


Fig. 3: A comparison of four captions generated by different methods for the same area: the base model (top left), OSMDA-Captions - the base model with provided OSM map (top right), the base fine-tuned on the training splits of benchmarks (bottom left), and OSMDA-VLM - the base jointly trained on OSMDA-Captions and training splits (bottom right). Methods are ranked based on the largest number of wins across all metrics and benchmarks, where benchmarking is possible. Joint training with our dataset stabilizes the model, resulting in less hallucination and better descriptions of spatial and visual layout. OSMDA-Captions also contain comparatively accurate descriptions with the help of the OSM map, yet qualitatively, not on the level of OSMDA-VLM. Both base and base-fine-tuned sometimes hallucinate: in this case, the base model incorrectly places the dome-shaped structure in the center, while base-fine-tuned hallucinates a nonexistent pond.

Captions [5], UCM-Captions [42], VRS Bench [23], RSVQA-HR, and RSVQA-LR [28]; and five where we do not consider a training split to measure generalization - AID [56], Million-AID [29], EuroSAT [13], XLRs-Bench [52] and SkyScript-Bench - the classification benchmark of SkyScript [55]. We call the first set the **fine-tuning-split**, and the second set the **generalization-split**. These datasets measure performance on various tasks: short captioning, detailed captioning, visual question answering (VQA), and scene classification. The VQAs also have different subtasks - object presence, counting, comparison, areas, classification of images, object types and textures. Both the fine-tuning and the generalization splits contain representatives of all tasks, but with differing objects, classes, formulations, and styles. Each task provides one of three forms of ground truth. For multiple-choice labels, we measure macro-averaged F1 score [49], as it is widely used to combine precision and recall into a single metric and is commonly reported in settings where class imbalance can make accuracy less informative. For numeric labels, we measure mean absolute error (MAE). To aggregate metrics across subtasks, we threshold MAE and normalize it before averaging (refer to Supplementary). For open-text answers, we measure G-Eval [27], a structured LLM-as-a-judge framework that improves robustness by deriving scores from next-token probability distributions instead of relying on a single sampled rating. We use *Qwen2.5-32B-Instruct* [59] as the judging model. All final scores are normalized to a scale of 0 to 1. For baselines, we select the most competitive models mentioned in Section 2 alongside Intern-S1-mini [3].

Table 2: Metrics across benchmarks. Metrics for RSVQA are aggregated. **Purple color** marks benchmarks whose training sets were used for fine-tuning of OSMDA-VLM (the fine-tuning-split – first five); **teal color** marks benchmarks where OSMDA-VLM evaluation is zero-shot (the generalization-split – last five). **Purple color** also marks results where the corresponding dataset has been included in the model’s training data in some way. Best metrics are highlighted in bold, top-3 metrics are underscored. Note that training data of Intern-S1-mini is not public, but it is also likely trained on some of the benchmarks.

Model	NWPU	UCM	RSVQA	RSVQA	VRSBench	AID	EuroSAT	SkyScript	Million	XLRS-Bench				
	Captions	Captions	LR	HR	caption			vqa	bench	AID	caption	vqa		
	<i>g_{eval}</i>	<i>g_{eval}</i>	agg	agg	<i>g_{eval}</i>			<i>g_{eval}</i>	fl	fl	fl	fl	<i>g_{eval}</i>	fl
GeoPix	0.072	0.145	0.177	0.322	0.000	0.379	0.054	0.058	0.006	0.000	0.000	0.001		
SkyEyeGPT	0.061	0.092	0.223	0.209	0.009	0.300	0.009	0.029	0.002	0.000	0.113	0.006		
GeoChat	0.181	0.179	0.690	0.412	0.157	0.382	0.559	0.369	0.316	0.079	0.021	0.010		
SkySenseGPT	0.177	0.179	0.656	0.477	0.221	0.38	0.706	0.445	0.394	0.145	0.100	0.012		
LRS-VQA	0.124	0.166	0.299	0.687	0.193	0.457	0.51	0.476	0.433	0.354	0.147	0.088		
VHM	0.308	0.375	0.554	0.460	0.177	0.536	0.748	0.362	0.546	0.094	0.216	0.011		
EarthDial	0.362	0.445	0.813	0.522	0.229	0.448	0.838	0.357	0.422	0.014	0.082	0.000		
LHRS-Bot-nova	0.281	0.286	0.618	0.600	0.144	0.543	0.789	0.466	0.523	0.306	0.111	0.039		
Intern-S1-mini	0.210	0.246	0.766	0.493	0.245	0.587	0.685	0.410	0.413	0.426	0.384	0.124		
OSMDA-VLM	0.395	0.500	0.806	0.725	0.429	0.744	0.670	0.449	0.507	0.504	0.404	0.216		

Main experiments. We select InternVL3_5-8B as the base model due to its strong performance in OCR tasks and various different domains [54]. For our main experiments, we train three variants: **ours**, where the base model is fine-tuned on OSMDA-Captions; **ours-joint-training (OSMDA-VLM)**, where it is fine-tuned on an equal-size mixture of OSMDA-Captions (200514 samples) and the fine-tuning-split training sets (200514 samples); and **base-fine-tuned**, where it is fine-tuned on 400000 samples from the fine-tuning-split only. When sampling from the fine-tuning-split, we balance the component datasets by sub-sampling larger datasets and repeating smaller ones so that each contributes the same number of training examples.

Ablations. We additionally conduct two ablations to isolate specific effects of the OSMDA method. To compare against the more traditional paradigm of distilling large and powerful teachers, we caption the images of OSMDA-Captions with *gemma-3-27b-it* [48] without providing the OSM maps and train the base model on these captions. We call the resulting model **teacher-ablation**. We also include the fine-tuning-split training sets with the same strategy as for ours-joint-training and train on the mixture, producing **teacher-ablation-joint-training**. Last, to determine whether the OSMDA method yields a model that is also better at picking up downstream tasks, we train ours sequentially on the fine-tuning-split (as opposed to training jointly), like for base-fine-tuned, producing **ours-fine-tuned**.

Experimental setup. We conduct each training with Low-Rank Adaptation (LoRA) [14], which adds trainable low-rank matrices to the original frozen weights, and set the LoRA ranks to 16, applying mild dropout regularization [46] with a 0.05 dropout probability. Trainings are carried out with mixed precision

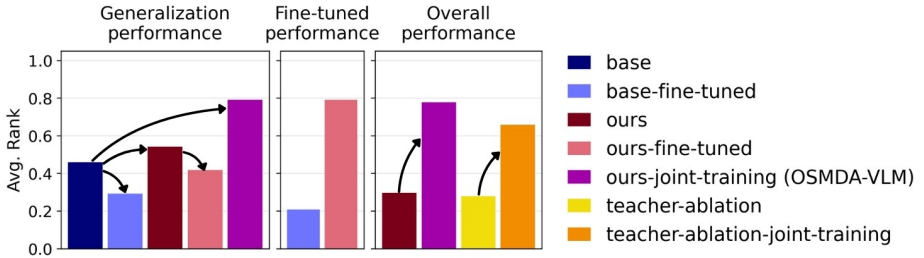


Fig. 4: Effects on performance of the OSMDA method. Each barplot shows the average rank when comparing benchmarking results between the included models across all metrics. The generalization barplot shows performance on benchmarks without considering training sets (generalization-split). Fine-tuned performance barplot shows performance on benchmarks with training splits that the models are fine-tuned on (fine-tuning-split). Overall performance includes both. OSMDA-VLM improves the generalization of the base model the most. Fine-tuning after training on OSMDA-Captions (ours-fine-tuned) also results in a model better at the downstream tasks compared to fine-tuning the base model directly. The gains of the OSMDA method outweigh even those of the standard method of distilling a large teacher, which is much more costly.

(bfloat16) on 16 NVIDIA H200 GPUs, with a total batch size of 32, a constant learning rate of 1×10^{-4} , and the AdamW optimizer [30] over one epoch.

We then benchmark the resulting models on the testing sets of all ten benchmark datasets, keeping the prompts fixed across models. For benchmarking details, refer to the supplementary material.

4.2 Results

OSMDA-VLM is state-of-the-art. Table 2 contains detailed benchmarking results. Compared to all baselines, OSMDA-VLM performs best on six out of ten benchmarks, and is in the top-3 on all benchmarks except one. Notably, some models deliver no correct responses on specific benchmarks, revealing limitations that become apparent under our evaluation (see section 5). In the zero-shot setting (the generalization-split), OSMDA-VLM outperforms all baselines on XLRs-Bench and Million-AID by a large margin. On EuroSAT and SkyScript-Bench it is in third place close to the best performers, and it fails to reach the top-3 only in AID.

The OSMDA method significantly improves the base model – even more than the standard of distilling a large teacher. Figure 4 showcases the effects of the OSMDA method. OSMDA-VLM (ours-joint-training) – the product of fine-tuning the base model on a mix of OSMDA-Captions and additional data (the fine-tuning-split) – results in a model that consistently generalizes better. Fine-tuning on downstream tasks after first training on OSMDA-Captions also results in better downstream performance compared to directly fine-tuning the base model. Last, training on captions generated by a much larger teacher (teacher-ablation) - gemma-3-27b-it - results in a model

significantly worse than training on captions generated by the student with the OSMDA method (ours). Mixing in the fine-tuning-split with the teacher-generated captions (teacher-ablation-joint-training) fails to change this trend, and OSMDA-VLM remains overall the best model. For detailed benchmarking results of these ablations, refer to the supplementary. A qualitative comparison is visible in Figure 3.

5 Discussion

OSMDA-VLM as state-of-the-art. Compared to all considered baselines, OSMDA-VLM is the only model that is consistently among the best models across benchmarks. Interestingly, even fine-tuning on downstream tasks after first training on OSMDA-Captions (ours-fine-tuned) yields higher downstream performance than directly fine-tuning the base model. This indicates that OSMDA-Captions acts as an effective intermediate training stage: it teaches transferable representations and priors, so the model starts downstream training from a better initialization and adapts more efficiently. OSMDA-VLM outperforms baselines by a very large margin in some of the most challenging benchmarks: RSVQA-HR, which requires understanding high-resolution, fine-grained detail; VRSBench and XLRBench, whose captions and VQAs are detailed, diverse, and require picking up elaborate spatial and visual cues in high- and extremely-high-resolutions; and Million-AID, which has over 50 classes. In the generalization setting, OSMDA-VLM remains consistently the strongest model despite not being exposed to most of the evaluation prompts during training. This indicates that its gains are not tied to memorizing particular templates, but reflect genuine robustness to unseen instructions – a property our experiments show is lacking in several baselines.

Instruction Brittleness in Baseline Models. A recurring pattern across our evaluation is sensitivity to instruction format – models, even if evaluated on benchmarks they have been trained on, degrade substantially when instructions are paraphrased. While this brittleness is present to some degree in all evaluated baselines, it is most pronounced in GeoPix and SkyEyeGPT. Both models are trained on corpora constructed partly through rule-based pipelines, which tend to produce a narrow and repetitive distribution of output formats. As a consequence, the models learn to condition their responses on superficial textual cues rather than on the underlying question semantics. This manifests most visibly in open-ended generation tasks: the models either produce responses in a rigid template that does not match the evaluation protocol, or they refuse to engage with the question at all - for example, GeoPix refuses to produce any captions with the unified VRSBench captioning prompt, resulting in a G-Eval of 0.0. This distinction between factual competence and instruction-following robustness has meaningful practical implications: a model deployed in a real system will encounter varied, user-generated prompts, and brittleness to format is therefore a genuine capability limitation, not a benchmarking artifact.

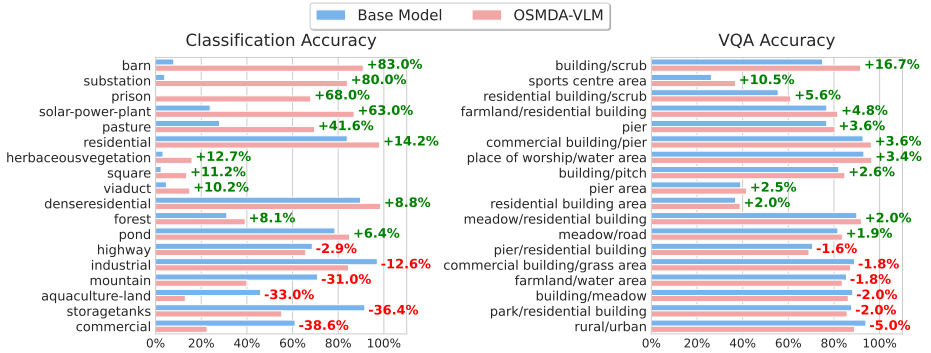


Fig. 5: Per-category accuracy for classification (left) and VQA (right). In the VQA panel, *rural/urban* denotes scene discrimination, while other slash-separated labels (e.g., *building/scrub*) indicate quantitative object comparison.

Map-Induced Biases. Because OSMDA-VLM learns directly from OpenStreetMap tiles, it naturally inherits the map’s representational features (Figure 5). Our pipeline generates precise captions for distinct, well-labeled infrastructure, yielding substantial classification gains for objects like barns and prisons, and improved VQA accuracy for clear boundaries like farmland adjacent to roads. However, in broad mixed-use areas where map annotations are inherently sparse, the resulting captions lack descriptive detail. Consequently, performance drops in complex environments, evidenced by classification degradations for commercial and industrial zones, and reduced VQA reliability for overlapping semantics like commercial buildings paired with parking. In practice, map-based supervision naturally focuses the model on areas with the most complete geographic data. OSMDA-VLM is also biased towards words common in the labels of the OSM maps (see Section 3.1), subsequently transferred to OSMDA-Captions, which sometimes affects its VQA performance negatively.

6 Conclusion

In this work, we introduce OSMDA, a fully self-contained domain adaptation framework for remote sensing VLMs that replaces expensive teacher-dependent pseudo-labeling with supervision extracted directly from OpenStreetMap. By rendering geo-aligned OSM tiles and leveraging the base model’s existing OCR and map/chart comprehension abilities, the model can label its own training data with detailed, geographically grounded captions, producing OSMDA-Captions at scale without manual annotation, proprietary APIs, or stronger external models. An extensive unified evaluation reveals that our OSMDA method improves both fine-tuned performance on downstream tasks and zero-shot generalization. Jointly mixing OSMDA-Captions with standard benchmark training splits yields OSMDA-VLM, which achieves state-of-the-art performance while remaining substantially cheaper and more scalable than frontier-teacher distillation pipelines.

Beyond raw performance, our evaluation also highlights pervasive instruction brittleness in prior RS-VLMs and shows that self-generated, map-grounded supervision can improve generalization while preserving instruction-following robustness. Overall, these results suggest that coupling strong foundation VLMs with crowd-sourced geographic data is a practical path to scalable remote sensing adaptation – turning freely available data into a durable substitute for costly human labels and brittle teacher models.

References

1. AI9Stars: Xlrs-bench: Benchmarking multimodal llms in ultra-high-resolution remote sensing. <https://github.com/AI9Stars/XLRS-Bench> (2025), gitHub repository 33
2. Andy Allan and contributors: OpenStreetMap Carto: A global map style for OpenStreetMap maps. <https://github.com/openstreetmap-carto/openstreetmap-carto>, <https://github.com/openstreetmap-carto/openstreetmap-carto> 3, 8, 25
3. Bai, L., Cai, Z., Cao, M., Cao, W., Chen, C., et al.: Intern-s1: A scientific multimodal foundation model (2025), <https://arxiv.org/abs/2508.15763> 2, 10
4. Chen, L., Li, J., Dong, X., Zhang, P., He, C., Wang, J., Zhao, F., Lin, D.: Sharegpt4v: Improving large multi-modal models with better captions. In: Computer Vision – ECCV 2024: 18th European Conference, Milan, Italy, September 29–October 4, 2024, Proceedings, Part XVII. p. 370–387. Springer-Verlag, Berlin, Heidelberg (2024). https://doi.org/10.1007/978-3-031-72643-9_22, https://doi.org/10.1007/978-3-031-72643-9_22 6
5. Cheng, Q., Huang, H., Xu, Y., Zhou, Y., Li, H., Wang, Z.: Nwpu-captions dataset and mlca-net for remote sensing image captioning. *IEEE Transactions on Geoscience and Remote Sensing* **60**, 1–19 (2022). <https://doi.org/10.1109/TGRS.2022.3201474> 10, 28
6. Dai, W., Li, J., Li, D., Tiong, A.M.H., Zhao, J., Wang, W., Li, B., Fung, P., Hoi, S.: Instructblip: towards general-purpose vision-language models with instruction tuning. In: Proceedings of the 37th International Conference on Neural Information Processing Systems. NIPS '23, Curran Associates Inc., Red Hook, NY, USA (2023) 4
7. Dong, X., Zhang, P., Zang, Y., Cao, Y., Wang, B., Ouyang, L., Zhang, S., Duan, H., Zhang, W., Li, Y., Yan, H., Gao, Y., Chen, Z., Zhang, X., Li, W., Li, J., Wang, W., Chen, K., He, C., Zhang, X., Dai, J., Qiao, Y., Lin, D., Wang, J.: Internlm-xcomposer2-4khd: A pioneering large vision-language model handling resolutions from 336 pixels to 4k hd. In: Globerson, A., Mackey, L., Belgrave, D., Fan, A., Paquet, U., Tomczak, J., Zhang, C. (eds.) *Advances in Neural Information Processing Systems*. vol. 37, pp. 42566–42592. Curran Associates, Inc. (2024). <https://doi.org/10.52202/079017-1348>, https://proceedings.neurips.cc/paper_files/paper/2024/file/4b06cdddb1cde6624c0be1465c7b800f-Paper-Conference.pdf 6
8. Dosovitskiy, A., Beyer, L., Kolesnikov, A., Weissenborn, D., Zhai, X., Unterthiner, T., Dehghani, M., Minderer, M., Heigold, G., Gelly, S., Uszkoreit, J., Houlsby, N.: An image is worth 16x16 words: Transformers for image recognition at scale. In: *International Conference on Learning Representations* (2021), <https://openreview.net/forum?id=YicbFdNTTy> 4

9. Drusch, M., Del Bello, U., Carlier, S., Colin, O., Fernandez, V., Gascon, F., Hoersch, B., Isola, C., Laberinti, P., Martimort, P., Meygret, A., Spoto, F., Sy, O., Marchese, F., Bargellini, P.: Sentinel-2: Esa's optical high-resolution mission for gmes operational services. *Remote Sensing of Environment* **120**, 25–36 (2012). <https://doi.org/10.1016/j.rse.2011.11.026> 6
10. Earth Resources Observation and Science (EROS) Center: National agriculture imagery program (naip) (2017). <https://doi.org/10.5066/F7QN651G>, <https://doi.org/10.5066/F7QN651G> 6
11. Feng, J., Luo, H., Gu, Z.: Improving semi-supervised remote sensing scene classification via multilevel feature fusion and pseudo-labeling. *International Journal of Applied Earth Observation and Geoinformation* **136**, 104335 (2025). <https://doi.org/https://doi.org/10.1016/j.jag.2024.104335>, <https://www.sciencedirect.com/science/article/pii/S1569843224006939> 5
12. Ge, J., Zhang, X., Zheng, Y., Guo, K., Liang, J.: Rsteller: Scaling up visual language modeling in remote sensing with rich linguistic semantics from openly available data and large language models. *ISPRS Journal of Photogrammetry and Remote Sensing* **226**, 146–163 (2025). <https://doi.org/https://doi.org/10.1016/j.isprsjprs.2025.05.002>, <https://www.sciencedirect.com/science/article/pii/S0924271625001832> 6
13. Helber, P., Bischke, B., Dengel, A., Borth, D.: Eurosat: A novel dataset and deep learning benchmark for land use and land cover classification. *IEEE Journal of Selected Topics in Applied Earth Observations and Remote Sensing* **12**(7), 2217–2226 (2019). <https://doi.org/10.1109/JSTARS.2019.2918242> 10, 28
14. Hu, E.J., yelong shen, Wallis, P., Allen-Zhu, Z., Li, Y., Wang, S., Wang, L., Chen, W.: LoRA: Low-rank adaptation of large language models. In: *International Conference on Learning Representations* (2022), <https://openreview.net/forum?id=nZvKeeFYf9> 11
15. Hu, Y., Yuan, J., Wen, C., Lu, X., Liu, Y., Li, X.: Rsgpt: A remote sensing vision language model and benchmark. *ISPRS Journal of Photogrammetry and Remote Sensing* **224**, 272–286 (2025). <https://doi.org/https://doi.org/10.1016/j.isprsjprs.2025.03.028>, <https://www.sciencedirect.com/science/article/pii/S0924271625001352> 2, 5
16. Jiang, A.Q., Sablayrolles, A., Roux, A., Mensch, A., Savary, B., Bamford, C., Chaplot, D.S., Casas, D.d.l., Hanna, E.B., Bressand, F., Lengyel, G., et al.: Mixtral of experts. *arXiv preprint arXiv:2401.04088* (2024) 6
17. Kage, P., Rothenberger, J.C., Andreadis, P., Diochnos, D.I.: A review of pseudo-labeling for computer vision (2025), <https://arxiv.org/abs/2408.07221> 5
18. Kuckreja, K., Danish, M.S., Naseer, M., Das, A., Khan, S., Khan, F.S.: Geochat: Grounded large vision-language model for remote sensing. In: *Proceedings of the IEEE/CVF Conference on Computer Vision and Pattern Recognition (CVPR)*. pp. 27831–27840 (June 2024) 2, 4, 5
19. Li, C., Wong, C., Zhang, S., Usuyama, N., Liu, H., Yang, J., Naumann, T., Poon, H., Gao, J.: LLaVA-med: Training a large language-and-vision assistant for biomedicine in one day. In: *Thirty-seventh Conference on Neural Information Processing Systems Datasets and Benchmarks Track* (2023), <https://openreview.net/forum?id=GSuP99u2kR> 4
20. Li, J., Li, D., Savarese, S., Hoi, S.: BLIP-2: Bootstrapping language-image pre-training with frozen image encoders and large language models. In: Krause, A., Brunskill, E., Cho, K., Engelhardt, B., Sabato, S., Scarlett, J. (eds.) *Proceedings of the 40th International Conference on Machine Learning*. *Proceedings of Machine*

- Learning Research, vol. 202, pp. 19730–19742. PMLR (23–29 Jul 2023), <https://proceedings.mlr.press/v202/li23q.html> 4
21. Li, K., Xin, Z., Pang, L., Pang, C., Deng, Y., Yao, J., Xia, G., Meng, D., Wang, Z., Cao, X.: Segearth-r1: Geospatial pixel reasoning via large language model (2025), <https://arxiv.org/abs/2504.09644> 5
 22. Li, W., Xiang, X., Wen, Z., Zhou, G., Niu, B., Wang, F., Huang, L., Wang, Q., Hu, Y.: Georeason: Aligning thinking and answering in remote sensing vision-language models via logical consistency reinforcement learning (2026), <https://arxiv.org/abs/2601.04118> 5
 23. Li, X., Ding, J., Elhoseiny, M.: Vrsbench: A versatile vision-language benchmark dataset for remote sensing image understanding. In: Globerson, A., Mackey, L., Belgrave, D., Fan, A., Paquet, U., Tomczak, J., Zhang, C. (eds.) *Advances in Neural Information Processing Systems*. vol. 37, pp. 3229–3242. Curran Associates, Inc. (2024). <https://doi.org/10.52202/079017-0106>, https://proceedings.neurips.cc/paper_files/paper/2024/file/05b7f821234f66b78f99e7803fffa78a-Paper-Datasets_and_Benchmarks_Track.pdf 10, 28
 24. Li, Z., Muhtar, D., Gu, F., He, Y., Zhang, X., Xiao, P., He, G., Zhu, X.: Lhrs-bot-nova: Improved multimodal large language model for remote sensing vision-language interpretation. *ISPRS Journal of Photogrammetry and Remote Sensing* **227**, 539–550 (2025). <https://doi.org/https://doi.org/10.1016/j.isprsjprs.2025.06.003>, <https://www.sciencedirect.com/science/article/pii/S0924271625002230> 2, 4, 5, 6
 25. Liu, H., Li, C., Wu, Q., Lee, Y.J.: Visual instruction tuning. In: *Advances in Neural Information Processing Systems (NeurIPS)* (2023) 4
 26. Liu, J., Sun, L., Fu, R., Yang, B.: Towards faithful reasoning in remote sensing: A perceptually-grounded geospatial chain-of-thought for vision-language models (2026), <https://arxiv.org/abs/2509.22221> 5
 27. Liu, Y., Iyer, D., Xu, Y., Wang, S., Xu, R., Zhu, C.: G-Eval: NLG evaluation using GPT-4 with better human alignment. In: Bouamor, H., Pino, J., Bali, K. (eds.) *Proceedings of the 2023 Conference on Empirical Methods in Natural Language Processing*. pp. 2511–2522. Association for Computational Linguistics, Singapore (Dec 2023). <https://doi.org/10.18653/v1/2023.emnlp-main.153>, <https://aclanthology.org> 10, 27, 28
 28. Lobry, S., Marcos, D., Murray, J., Tuia, D.: Rsvqa: Visual question answering for remote sensing data. *IEEE Transactions on Geoscience and Remote Sensing* **58**(12), 8555–8566 (2020). <https://doi.org/10.1109/TGRS.2020.2988782> 10, 28
 29. Long, Y., Xia, G.S., Li, S., Yang, W., Yang, M.Y., Zhu, X.X., Zhang, L., Li, D.: On creating benchmark dataset for aerial image interpretation: Reviews, guidances, and million-aid. *IEEE Journal of Selected Topics in Applied Earth Observations and Remote Sensing* **14**, 4205–4230 (2021). <https://doi.org/10.1109/JSTARS.2021.3070368> 10, 28
 30. Loshchilov, I., Hutter, F.: Decoupled weight decay regularization. preprint arXiv:1711.05101 (2017) 12
 31. Luo, J., Pang, Z., Zhang, Y., Wang, T., Wang, L., Dang, B., Lao, J., Wang, J., Chen, J., Tan, Y., Li, Y.: Skysensegpt: A fine-grained instruction tuning dataset and model for remote sensing vision-language understanding (2024), <https://arxiv.org/abs/2406.10100> 4, 5
 32. Luo, J., Zhang, Y., Yang, X., Wu, K., Zhu, Q., Liang, L., Chen, J., Li, Y.: When large vision-language model meets large remote sensing imagery: Coarse-to-fine

- text-guided token pruning. In: Proceedings of the IEEE/CVF International Conference on Computer Vision (ICCV). pp. 9206–9217 (October 2025) 4
33. Markov, M., Ailuro, S.M., Gool, L.V., Schindler, K., Paudel, D.P.: Firescope: Wildfire risk prediction with a chain-of-thought oracle (2025), <https://arxiv.org/abs/2511.17171> 5
 34. Moslemi, A., Briskina, A., Dang, Z., Li, J.: A survey on knowledge distillation: Recent advancements. *Machine Learning with Applications* **18**, 100605 (2024). <https://doi.org/https://doi.org/10.1016/j.mlwa.2024.100605>, <https://www.sciencedirect.com/science/article/pii/S2666827024000811> 5
 35. Muhtar, D., Li, Z., Gu, F., Zhang, X., Xiao, P.: Lhrs-bot: Empowering remote sensing with vgi-enhanced large multimodal language model. In: Leonardis, A., Ricci, E., Roth, S., Russakovsky, O., Sattler, T., Varol, G. (eds.) *Computer Vision – ECCV 2024*. pp. 440–457. Springer Nature Switzerland, Cham (2025) 5
 36. OpenAI: Gpt-4 technical report (2023), <https://arxiv.org/abs/2303.08774> 2, 6
 37. OpenAI: Gpt-4o system card. Tech. rep., OpenAI (2024), <https://openai.com/index/gpt-4o-system-card/>, accessed: 2025-03-05 5
 38. OpenStreetMap contributors: Planet dump retrieved from <https://planet.osm.org>. <https://www.openstreetmap.org> (2025) 3, 6, 21
 39. Ou, R., Hu, Y., Zhang, F., Chen, J., Liu, Y.: Geopix: A multimodal large language model for pixel-level image understanding in remote sensing. *IEEE Geoscience and Remote Sensing Magazine* **13**(3), 324–337 (2025). <https://doi.org/10.1109/MGRS.2025.3560293> 2, 4, 5
 40. Pang, C., Weng, X., Wu, J., Li, J., Liu, Y., Sun, J., Li, W., Wang, S., Feng, L., Xia, G.S., He, C.: Vhm: Versatile and honest vision language model for remote sensing image analysis. Proceedings of the AAAI Conference on Artificial Intelligence **39**(6), 6381–6388 (Apr 2025). <https://doi.org/10.1609/aaai.v39i6.32683>, <https://ojs.aaai.org/index.php/AAAI/article/view/32683> 2, 4, 5, 6
 41. Pavlenko, A., The Mapnik Contributors: Mapnik: Open Source Toolkit for Developing Mapping Applications. Mapnik Project (11 2025), <https://mapnik.org/>, version 4.1.4 3, 8
 42. Qu, B., Li, X., Tao, D., Lu, X.: Deep semantic understanding of high resolution remote sensing image. In: 2016 International Conference on Computer, Information and Telecommunication Systems (CITS). pp. 1–5 (2016). <https://doi.org/10.1109/CITS.2016.7546397> 10, 28
 43. Radford, A., Kim, J.W., Hallacy, C., Ramesh, A., Goh, G., Agarwal, S., Sastry, G., Askell, A., Mishkin, P., Clark, J., Krueger, G., Sutskever, I.: Learning transferable visual models from natural language supervision. In: Meila, M., Zhang, T. (eds.) Proceedings of the 38th International Conference on Machine Learning. Proceedings of Machine Learning Research, vol. 139, pp. 8748–8763. PMLR (18–24 Jul 2021), <https://proceedings.mlr.press/v139/radford21a.html> 4
 44. Siméoni, O., Vo, H.V., Seitzer, M., Baldassarre, F., Oquab, M., Jose, C., Khalidov, V., Szafraniec, M., Yi, S., Ramamonjisoa, M., Massa, F., Haziza, D., Wehrstedt, L., Wang, J., Darcet, T., Moutakanni, T., Sentana, L., Roberts, C., Vedaldi, A., Tolan, J., Brandt, J., Couprie, C., Mairal, J., Jégou, H., Labatut, P., Bojanowski, P.: DINOv3 (2025), <https://arxiv.org/abs/2508.10104> 8, 25
 45. Soni, S., Dudhane, A., Debary, H., Fiaz, M., Munir, M.A., Danish, M.S., Fraccaro, P., Watson, C.D., Klein, L.J., Khan, F.S., Khan, S.: Earthdial: Turning multi-sensory earth observations to interactive dialogues. In: Proceedings of the IEEE/CVF Conference on Computer Vision and Pattern Recognition (CVPR). pp. 14303–14313 (June 2025) 4, 5, 6

46. Srivastava, N., Hinton, G., Krizhevsky, A., Sutskever, I., Salakhutdinov, R.: Dropout: A simple way to prevent neural networks from overfitting. *Journal of Machine Learning Research* **15**, 1929–1958 (2014) 11
47. Team, G., et al.: Gemini: A family of highly capable multimodal models. arXiv preprint arXiv:2312.11805 (2023), <https://arxiv.org/abs/2312.11805> 2, 6
48. Team, G., Kamath, A., Ferret, J., Pathak, S., Vieillard, N., Merhej, R., Perrin, S., Matejovicova, T., Ramé, A., Rivière, M., Rouillard, L., Mesnard, T., Cideron, G., Grill, J.B., Ramos, S., Yvinec, E., Casbon, M., Pot, E., Penchev, I., Liu, G., Visin, F., Kenealy, K., Beyer, L., Zhai, X., Tsitsulin, A., Busa-Fekete, R., Feng, A., Sachdeva, N., Coleman, B., Gao, Y., Mustafa, B., Barr, I., Parisotto, E., Tian, D., Eyal, M., Cherry, C., Peter, J.T., Sinopalnikov, D., Bhupatiraju, S., Agarwal, R., Kazemi, M., Malkin, D., Kumar, R., Vilar, D., Brusilovsky, I., Luo, J., Steiner, A., Friesen, A., Sharma, A., Sharma, A., Gilady, A.M., et al.: Gemma 3 technical report. arXiv preprint arXiv:2503.19786 (2025), <https://arxiv.org/abs/2503.19786> 11
49. Van Rijsbergen, C.J.: *Information Retrieval*. Butterworths, London (1979), <https://www.dcs.gla.ac.uk/Keith/Preface.html> 10
50. Wada, Y., Kaneda, K., Saito, D., Sugiura, K.: Polos: Multimodal metric learning from human feedback for image captioning. In: *Proceedings of the IEEE/CVF Conference on Computer Vision and Pattern Recognition (CVPR)*. pp. 13559–13568 (June 2024) 28
51. Wang, D., Liu, S., Jiang, W., Wang, F., Liu, Y., Qin, X., Luo, Z., Zhou, C., Guo, H., Zhang, J., Du, B., Tao, D., Zhang, L.: Geozero: Incentivizing reasoning from scratch on geospatial scenes (2026), <https://arxiv.org/abs/2511.22645> 5
52. Wang, F., Wang, H., Guo, Z., Wang, D., Wang, Y., Chen, M., Ma, Q., Lan, L., Yang, W., Zhang, J., Liu, Z., Sun, M.: Xlrs-bench: Could your multimodal llms understand extremely large ultra-high-resolution remote sensing imagery? In: *Proceedings of the IEEE/CVF Conference on Computer Vision and Pattern Recognition (CVPR)*. pp. 14325–14336 (June 2025) 2, 10, 28
53. Wang, L., Yoon, K.J.: Knowledge Distillation and Student-Teacher Learning for Visual Intelligence: A Review and New Outlooks . *IEEE Transactions on Pattern Analysis & Machine Intelligence* **44**(06), 3048–3068 (Jun 2022). <https://doi.org/10.1109/TPAMI.2021.3055564>, <https://doi.ieeecomputersociety.org/10.1109/TPAMI.2021.3055564> 5
54. Wang, W., Gao, Z., Gu, L., Pu, H., Cui, L., Wei, X., Liu, Z., Jing, L., Ye, S., Shao, J., et al.: Internvl3.5: Advancing open-source multimodal models in versatility, reasoning, and efficiency. arXiv preprint arXiv:2508.18265 (2025). <https://doi.org/10.48550/arXiv.2508.18265>, <https://arxiv.org/abs/2508.18265> 4, 11
55. Wang, Z., Prabha, R., Huang, T., Wu, J., Rajagopal, R.: Skyscript: a large and semantically diverse vision-language dataset for remote sensing. In: *Proceedings of the Thirty-Eighth AAAI Conference on Artificial Intelligence and Thirty-Sixth Conference on Innovative Applications of Artificial Intelligence and Fourteenth Symposium on Educational Advances in Artificial Intelligence. AAAI'24/IAAI'24/EAAI'24*, AAAI Press (2024). <https://doi.org/10.1609/aaai.v38i6.28393>, <https://doi.org/10.1609/aaai.v38i6.28393> 6, 7, 10, 28
56. Xia, G.S., Hu, J., Hu, F., Shi, B., Bai, X., Zhong, Y., Zhang, L., Lu, X.: Aid: A benchmark data set for performance evaluation of aerial scene classification. *IEEE Transactions on Geoscience and Remote Sensing* **55**(7), 3965–3981 (2017). <https://doi.org/10.1109/TGRS.2017.2685945> 10, 28

57. Xu, H., Xie, S., Tan, X., Huang, P.Y., Howes, R., Sharma, V., Li, S.W., Ghosh, G., Zettlemoyer, L., Feichtenhofer, C.: Demystifying CLIP data. In: The Twelfth International Conference on Learning Representations (2024), <https://openreview.net/forum?id=5BCF1nfE1g> 8, 25
58. Xue, X., Wei, G., Chen, H., Zhang, H., Lin, F., Shen, C., Zhu, X.X.: Reo-vlm: Transforming vlm to meet regression challenges in earth observation (2024), <https://arxiv.org/abs/2412.16583> 5
59. Yang, A., Yang, B., Zhang, B., Hui, B., Zheng, B., Yu, B., Li, C., Liu, D., Huang, F., Wei, H., Lin, H., Yang, J., Tu, J., Zhang, J., Yang, J., Yang, J., Zhou, J., Lin, J., Dang, K., Lu, K., Bao, K., Yang, K., Yu, L., Li, M., Xue, M., Zhang, P., Zhu, Q., Men, R., Lin, R., Li, T., Xia, T., Ren, X., Ren, X., Fan, Y., Su, Y., Zhang, Y., Wan, Y., Liu, Y., Cui, Z., Zhang, Z., Qiu, Z.: Qwen2.5 technical report. arXiv preprint arXiv:2412.15115 (2024) 8, 10, 24, 28
60. Yuan, Z., Xiong, Z., Mou, L., Zhu, X.X.: Chatearthnet: a global-scale image–text dataset empowering vision–language geo-foundation models. *Earth System Science Data* **17**(3), 1245–1263 (2025). <https://doi.org/10.5194/essd-17-1245-2025>, <https://essd.copernicus.org/articles/17/1245/2025/> 6
61. Zanaga, D., Van De Kerchove, R., Daems, D., De Keersmaecker, W., Brockmann, C., Kirches, G., Wevers, J., Cartus, O., Santoro, M., Fritz, S., Lesiv, M., Herold, M., Tsendbazar, N., Xu, P., Ramoino, F., Arino, O.: ESA WorldCover 10 m 2021 v200 (2022). <https://doi.org/10.5281/zenodo.7254221>, <https://doi.org/10.5281/zenodo.7254221> 6
62. Zhan, Y., Xiong, Z., Yuan, Y.: Skyeyegpt: Unifying remote sensing vision-language tasks via instruction tuning with large language model. *ISPRS Journal of Photogrammetry and Remote Sensing* **221**, 64–77 (2025). <https://doi.org/https://doi.org/10.1016/j.isprsjprs.2025.01.020>, <https://www.sciencedirect.com/science/article/pii/S0924271625000206> 2, 4, 5
63. Zhang, W., Cai, M., Zhang, T., Zhuang, Y., Mao, X.: Earthgpt: A universal multimodal large language model for multisensor image comprehension in remote sensing domain. *IEEE Transactions on Geoscience and Remote Sensing* **62**, 1–20 (2024). <https://doi.org/10.1109/TGRS.2024.3409624> 2
64. Zhou, B., Hu, Y., Weng, X., Jia, J., Luo, J., Liu, X., Wu, J., Huang, L.: Tinyllava: A framework of small-scale large multimodal models. arXiv preprint arXiv:2402.14289 (2024), <https://arxiv.org/abs/2402.14289> 5
65. Zhu, D., Chen, J., Shen, X., Li, X., Elhoseiny, M.: Minigpt-4: Enhancing vision-language understanding with advanced large language models. arXiv preprint arXiv:2304.10592 (2023) 4

Supplementary Material

7 Detailed Benchmarking Results

Detailed ablation results are reported in Table 3. Detailed performance on RSVQA is reported in Table 4 for both baselines and ablations.

Moreover, because RSVQA images are georeferenced which allows creation of corresponding OSM maps, we also evaluate our teacher – base with a map. It performs worse than base in RSVQA LR as fine-grained objects in very low-resolution images are too dense to label meaningfully, and therefore, mostly introduces biases; and it performs better than base in RSVQA HR. These dynamics are correlated with students’ performance improvements, as expected.

Table 3: Metrics across benchmarks for ablation models. ft stands for fine-tuned, jt stands for joint-training. Metrics for RSVQA are aggregated. **Purple color** marks benchmarks whose training sets were used for fine-tuning of OSMDA-VLM (the fine-tuning-split – first five); **teal color** marks benchmarks where OSMDA-VLM evaluation is zero-shot (the generalization-split – last five). **Purple color** also marks results where the corresponding dataset has been included in the model’s training data in some way. Best metrics are highlighted in bold, top-3 metrics are underscored.

Model	NWPU	UCM	RSVQA	RSVQA	VRSBench		AID	EuroSAT	SkyScript	Million	XLRs-Bench	
	Captions	Captions	LR	HR	caption	vqa	f1	f1	bench	AID	caption	vqa
	<i>geval</i>	<i>geval</i>	agg	agg	<i>geval</i>	<i>geval</i>			f1	f1	<i>geval</i>	f1
base	0.216	0.220	0.796	0.474	0.243	0.568	0.695	<u>0.416</u>	0.375	0.427	0.411	0.095
base-ft	0.412	0.507	0.823	0.747	0.434	0.755	0.695	0.406	0.375	0.402	0.326	<u>0.11</u>
ours	0.236	0.275	0.664	0.497	0.19	0.601	0.671	<u>0.444</u>	0.472	0.477	0.399	0.104
ours-ft	0.410	0.515	0.838	0.753	0.436	0.758	<u>0.705</u>	0.373	0.412	0.352	0.341	<u>0.164</u>
ours-jt	0.395	0.500	0.806	0.725	0.429	0.744	0.670	0.449	0.507	0.504	0.404	0.216
teacher-ablation	0.250	0.280	0.598	0.470	0.167	0.622	0.717	0.383	0.498	0.564	0.280	0.038
teacher-ablation-jt	0.385	0.529	0.820	0.731	0.418	0.738	<u>0.701</u>	0.373	<u>0.497</u>	<u>0.524</u>	0.234	0.084

8 Qualitative Examples

See qualitative examples of OSMDA-VLM vs baselines over XLRs-Bench at captioning in Figure 7 and vqa in Figure 6.

9 OSMDA-captions Details

OSMDA-captions and map generation consists of several major stages: data acquisition from the OpenStreetMap database [38], heuristic-based filtration, relabeling, distribution balancing, map rendering, captioning.

Filtration. First, OSM objects are acquired in raw tags format - a set of key-value pairs - and attached corresponding geometries. Acquired objects are typed by presence of keys: `amenity`, `highway`, `barrier`, `waterway`, `traffic_calming`,



Fig. 6: Two examples of VQAs from XLRS-Bench, with each model’s corresponding answers. Wrong format answers are colored grey, correct format wrong answers are colored red, and right answers are in green.

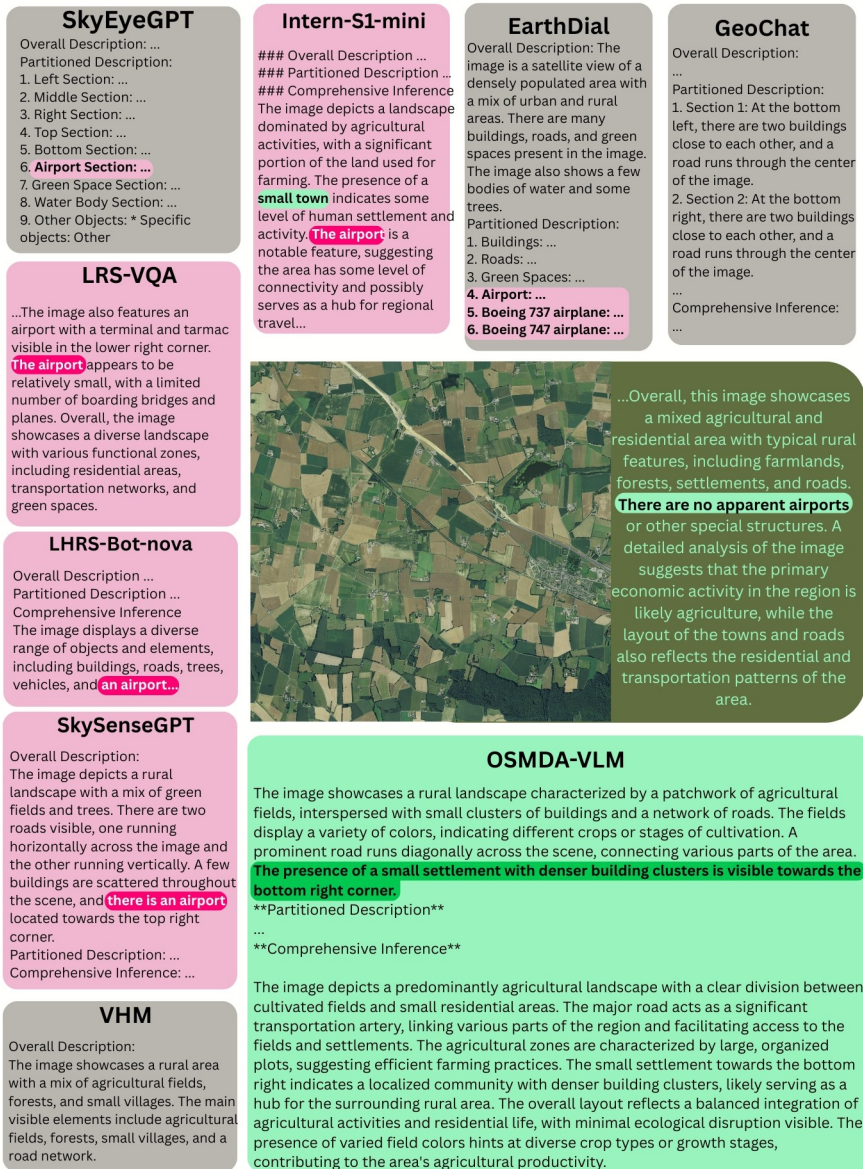


Fig. 7: A captioning example from XLRs-Bench. GeoPix is omitted as it produces empty output. Wrong format answers are colored grey, correct format wrong answers are colored red, and right answers are in green. Ellipses indicate trimmed content. VHM, SkyEyeGPT, EarthDial and GeoChat refuse to follow the official XLRs-Bench captioning prompt, which asks to split the image into nine quadrants. Many models hallucinate an airport. OSMDA-VLM does not hallucinate, and correctly identifies the settlement with proper spatial identification – something only Intern-S1-mini briefly mentions.

Table 4: Detailed performance on RSVQA and aggregate metrics for baselines and ablations. We also include our teacher’s predictions – base with a map. ft stands for fine-tuned, jt stands for joint-training.

model	RSVQA LR					RSVQA HR				
	rural-urban	presence	count	comparison	agg	presence	count	area, m^2	comparison	agg
	f1	f1	MAE	f1		f1	MAE	MAE	f1	
GeoPix	0.494	0.201	1552	0.011	0.177	0.556	2.39	1301	0.078	0.322
SkyEyeGPT	0.537	0.317	186	0.038	0.223	0.236	3.16	1301	0.098	0.209
GeoChat	0.905	0.938	134	0.816	0.690	0.618	3.94	1302	0.687	0.412
SkySenseGPT	0.687	0.913	109	0.752	0.656	0.581	2.06	1301	0.607	0.477
LRS-VQA	0.357	0.307	184	0.533	0.299	0.872	0.92	1200	0.860	0.687
VHM	0.843	0.682	184	0.691	0.554	0.687	2.16	1300	0.454	0.460
EarthDial	0.894	0.947	72	0.891	0.813	0.673	1.20	1301	0.684	0.522
LHRS-Bot-nova	0.629	0.897	133	0.837	0.618	0.785	1.33	1289	0.741	0.600
Intern-S1-mini	0.875	0.900	87	0.875	0.766	0.652	2.05	2396	0.731	0.493
base	0.941	0.879	74	0.861	0.796	0.678	2.57	7705	0.733	0.474
base with a map	0.889	0.870	76	0.851	0.776	0.712	1.94	112648	0.745	0.517
base-ft	0.935	0.942	67	0.869	0.823	0.899	1.08	832	0.860	0.747
ours	0.850	0.915	145	0.862	0.664	0.639	1.90	1317699	0.730	0.497
ours-ft	0.946	0.946	60	0.867	0.838	0.902	1.05	814	0.863	0.753
ours-jt (OSMDA-VLM)	0.867	0.941	66	0.858	0.806	0.890	1.07	921	0.839	0.725
teacher-ablation	0.686	0.845	135	0.761	0.598	0.638	2.21	191626	0.684	0.470
teacher-ablation-jt	0.899	0.943	63	0.859	0.820	0.885	1.09	869	0.837	0.731

building, man_made, natural, emergency, leisure, landuse, surface, route. Then, objects are filtered based on a set of visibility heuristics:

- geometry is polygon and its area is less than the area of a pixel;
- geometry is linestring and its length is less than the size of a pixel;
- one of subway, pipeline, cable, power cable, sewer, culvert, manhole is present in type values;
- or one of the key-value pairs location=underground, tunnel=yes, tunnel=culvert covered=yes, indoor=yes, parking=underground is present in tags.

Relabeling. Next, for each of the remaining objects, we process its tags with Qwen2.5-72B-Instruct [59], instructing it to produce a brief descriptive label by following prompt:

You are given data about an OpenStreetMap object (tags + geometry hints). Generate a short label.

Hard rules:

- Output a maximum of three words.
- No toponyms (no proper names, place names, brand names).
- No colors.
- Use only information explicitly present in the provided data.
- The label must reflect only what is reasonably identifiable from an overhead satellite image.
- The last word must be the primary physical object type (noun).
- Output only the label.

Known object properties: <key>: <value>, ...

where `<key>: <value>, ...` is the list of tags. This results in a total of 75k unique semantic tags.

Distribution balancing. At this stage, each RGB image is co-registered with set of objects, described by their labels and geometries. Balancing is performed based on three features in steps: semantic labels included in the image weighted by number of their occurrences; total number of objects in the image; perceptual embedding of the image itself for deduplication.

Balancing is performed based on the MetaCLIP [57] algorithm with magical numbers $t_1 = 700$ for the first step and $t_2 = 4000$ for the second. For the third step, DINOv3 [44] embeddings of the images are computed and projected into 256-dimensional space via PCA, and clustered with K-means into 25000 clusters, then balancing is applied with $t_3 = 15$. Magic number t stands for approximate expected number of images for each query, where queries are either unique semantic tags, bin of total number of objects in the image, or cluster assignment. Stages are applied consequently, so each stage is conditioned on the previous one, mitigating overcorrecting. Curation results in a set of 200514 images with 17.6 million objects and 47984 unique semantic tags.

Data sources contain imperfections: satellite imagery has instrumental errors, and OSM, being crowd-sourced, is inherently noisy. Even after curation some artifacts persist (see Figure 8a). Several images are partially corrupted, and several regions don't contain sufficient annotation. Nevertheless, the majority of the curated dataset is of high quality.

Map rendering. Maps are rendered via OpenStreetMap-carto [2] from filtered objects with names replaced by llm-produced labels. See Figure 8b for examples of images with corresponding maps of filtered OSM objects before and after relabeling. Toponyms and addresses are removed, and previously unnamed objects are labeled by their semantic tag. Final maps are dense and semantically rich while still readable.

Captioning. To generate OSMDA-Captions we prompt InternVL3.5-8B providing both satellite image and map as context. Note that map is used only at the data generation step and completely omitted during training. The prompt for captioning is as follows:

Task

Generate a single-paragraph, dense, highly detailed caption describing the aerial scene shown.

Inputs

You are provided with two satellite images of the same area:

1. An RGB aerial image.
2. The same image with a map overlay where objects are outlined and textually identified for reference only.

Mandatory Rules (Follow Exactly)

- Describe only what is visible from a top-down, aerial perspective, given the `<res> m` resolution.
- Use only visual evidence from the RGB image and the provided map.
- Do NOT infer, speculate, or guess. Avoid all uncertainty or hedging language.

- Do NOT use words or phrases such as: possibly, likely, appears, suggests, indicates, may, might.
- Do NOT reference the map, overlay, outlines, annotations, text, colors, or any labeling system in any way.
- Do NOT mention words such as: map, label, labeled, marked, outlined, annotation, legend.
- The provided object identifiers exist only to help you recognize features and must never appear in the caption.

Content Requirements

- Include every visible element present in the RGB image.
- Clearly and precisely describe spatial relationships, orientation, adjacency, alignment, density, and layout.
- Use a confident, declarative tone throughout.
- Write one single paragraph only.
- Be compact but information-dense; do not use bullet points or lists.

Output

Produce exactly one paragraph describing the scene in full detail, strictly adhering to all rules above.

where <res> is substituted by resolution in meters per pixel.

10 Benchmarking Details

10.1 Benchmarks

The benchmarks are selected to cover urban-focused scene understanding in various image sizes (64x64 to 10000x11500), resolutions (0.1 to 153 meters per pixel), instruction formats and tasks to achieve thorough evaluation of remote sensing VLMs; details are reported in Table 5. Part of the benchmarks were used for fine-tuning by baseline models, and part were evaluated before, the detailed correspondence is reported in Table 6.

10.2 Metrics

RSVQA agg. To calculate the aggregated performance in RSVQA we first reverse, normalize, and clip MAE: $nMAE = \max((M - MAE)/M, 0) \in [0, 1]$ with $M = 5$ for counting in RSVQA HR, $M = 150$ for counting in RSVQA LR, and $M = 1500$ for area. Finally, we average f1 and nMAE scores across all four tasks to get a single metric.

***g_{eval}* metric.** To assess the quality of the generated captions and open-ended answers, we employ G-Eval [27], a Large Language Model (LLM)-based evaluation framework. The framework extracts raw logits for the valid score tokens ("1" to "5") at the final sequence position. It then applies a softmax function, normalizes the probabilities across the tokens, and computes a weighted sum to yield a continuous score between 1.0 and 5.0. Finally, the raw scores are divided

Table 5: Description of benchmarks used in the study. VRSBench and XLRB-Bench also contain visual grounding task, which was omitted in the study. Images in RSVQA are georeferenced, which also allows to evaluate base with maps, i.e. teacher in OSMDA. Resolutions for VRSBench and XLRB-Bench were not reported before, we estimate it visually.

Benchmark	Task	Image sizes	Res, m/pixel	Note
AID [56]	cls	600x600	0.5 - 8	30 classes
EuroSAT [13]	cls	64x64	10-60	10 classes
SkyScript [55]	cls	77x77 - 1015x1084	0.1 - 30	70 classes, constructed from OSM tags
Million-AID [29]	cls	256x256, 512x512	0.5 - 153	hierarchical structure of 8/28/51 classes
UCM-Captions [42]	cap	256x256	0.3	short rigid-form captions
NWPU-Captions [5]	cap	256x256	0.2 - 30	short rigid-form captions
RSVQA LR [28]	vqa	256x256	10	rigid-form vqa, counting, area measurement
RSVQA HR [28]	vqa	512x512	0.15	rigid-form vqa and counting
VRSBench [23]	cap, vqa	512x512	0.1 - 1	open-ended vqa and detailed captions
XLRB-Bench [52]	cap, vqa	1169x1361 - 10000x11500	0.1 - 1	vqa and detailed captions

Table 6: The map of previous evaluations. FT marks whether the model was finetuned on the dataset, ZS stated whether the model was evaluated in zero-shot manner, x states that model was not evaluated before. Note that training data of Intern-S1-mini is not public, but it is also likely trained on some of the benchmarks.

Paper	AID	Euro SAT	Million AID	SkyScript bench	RSVQA LR	RSVQA HR	UCM Captions	NWPU Captions	VRS Bench	XLRB Bench
GeoPix	x	x	x	x	x	x	x	x	FT	x
SkyEyeGPT	x	x	x	x	FT	FT	FT	FT	x	x
GeoChat	ZS	x	x	x	FT	x	x	x	x	x
SkySenseGPT	ZS	x	x	x	FT	ZS	x	x	x	x
LRS-VQA	x	x	x	x	x	FT	x	x	x	x
VHM	ZS	x	x	x	FT	ZS	FT	FT	x	x
EarthDial	FT	FT	x	x	FT	FT	FT	FT	x	x
LHRS-Bot-nova	ZS	ZS	x	x	FT	FT	x	FT	x	x
Intern-S1-mini	x	x	x	x	x	x	x	x	x	ZS
ours	ZS	ZS	ZS	ZS	FT	FT	FT	FT	FT	ZS

by 5 to normalize them to $[0,1]$. The evaluation strictly compares predictions to the ground truth. It penalizes hallucinations and verifies object accuracy and counts.

Specifically, we utilize *Qwen2.5-32B-Instruct* [59] as our evaluator model. To decrease resource requirements, we omit the original Chain-of-Thought reasoning steps, so the judge model’s prediction is done in one forward pass. Following original paper, we validate our G-Eval setup by comparing it against human judgments on the Polaris dataset [50]. Across 26,122 samples, our setup aligns closely with human scores. We achieve Pearson (**0.632**), Spearman (**0.628**), and Kendall’s τ_c (**0.531**) (the primary metric in [50]) correlations, overcoming or comparable with results reported in the paper [27].

The exact prompt templates utilized for evaluations are provided below:

[Captions Prompt]

You are an expert judge evaluating satellite image captions. Your task is to compare the Predicted caption against the Ground Truth (GT) and assign a score based on object accuracy, counting, and hallucinations.

Evaluation Steps:

1. Analyze the Ground Truth for core objects and counts.
2. Check the Prediction for “Imaginary Objects” (Hallucinations) not present in the GT.
3. Verify if object counts and spatial relationships match the GT.
4. Assign a strict score from 1-5 using the rubric below.

Scoring Rubric:

- 1 (Critical Failure): Major hallucination (imaginary objects) or completely wrong scene classification.
- 2 (Poor): Correct scene type, but severe errors in object counting or wrong object attributes.
- 3 (Fair): Captures the main gist, but has minor hallucinations or noticeable counting errors.
- 4 (Good): Accurate objects and counts, with only very minor semantic differences or missing fine details.
- 5 (Perfect): Exact match in object types, counts, and spatial layout with no hallucinations.

Input:

Ground Truth: <gt>

Predicted: <pred>

Score:

[Open-Ended Questions / VQA Prompt]

You are an expert judge evaluating Visual Question Answering (VQA) outputs. Your task is to compare the Predicted Answer against the Ground Truth (GT) Answer for the given Question and assign a score based on factual correctness, completeness, and hallucinations.

Evaluation Steps:

1. Analyze the Question to understand what information is required.
2. Examine the Ground Truth Answer for key facts, values, and constraints.
3. Check the Predicted Answer for hallucinations (information not supported by the GT).
4. Verify correctness, precision, and completeness of the Predicted Answer.
5. Assign a strict score from 1-5 using the rubric below.

Scoring Rubric:

- 1 (Critical Failure): Incorrect answer or major hallucination; does not address the question.
- 2 (Poor): Partially related but mostly incorrect; major factual errors or missing key elements.
- 3 (Fair): Captures the general idea but contains minor errors, ambiguity, or incomplete details.

4 (Good): Mostly correct and complete; only very minor inaccuracies or omissions.

5 (Perfect): Exact match with the Ground Truth; fully correct, precise, and no hallucinations.

Input:

Question: <q>

Ground Truth Answer: <gt>

Predicted Answer: <pred>

Score: Where <q>, <gt>, and <pred> stand for the question, ground truth, and evaluated model’s prediction respectively.

10.3 Protocol

To benchmark each model, we tailor custom prompts for the combinations of datasets and tasks. We then generate each model’s deterministic predictions by sampling its highest likelihood tokens given the prompts. For each benchmark and task combination, we limit the maximum number of new tokens based on the semantic of the task. Below, we list the detailed configurations across datasets and benchmarks. We believe this makes our extensive evaluation fully reproducible, thus bringing the community closer to a unified benchmarking protocol where remote-sensing models can be unambiguously compared without having to re-implement the baselines of previous works. Note that across all zero-shot datasets, OSMDA-VLM has not seen any prompts during training, ensuring a genuine evaluation of its generalization capabilities.

NWPU-Captions and UCM-Captions. Both datasets have short captions very similar in structure. For both, generation is limited to a maximum of 128 new tokens, and they share the same prompt:

Task: Generate a single, strict-format caption for this satellite image.

Rules:

1. Output MUST be a single sentence under 15 words.
2. Do NOT use phrases like "The image shows" or "In this picture".
3. Do NOT describe surroundings, colors, or lighting.
4. Select ONE of the following sentence patterns based on the image content:

Pattern A (For Land/Terrain):

"There is a piece of terrain."

Pattern B (For Vehicles/Objects):

"Quantity objects are stopped/parked arrangement at the location."

(Note: Use "dispersedly" or "neatly" for arrangement).

Pattern C (For Facilities/Structures):

"It is a facility compose of materials."

(Note: Use the exact phrase "compose of").

Examples:

Input:

Output: There is a piece of desert.

Input:

Output: Many small boats are stopped neatly at the harbor.

Input:

Output: It is a tennis court compose of clay and white lines.

Input: [Target Image]

Output:

RSVQA-LR and RSVQA-HR. Both datasets have a predefined set of question types. *Presence, counting and comparison* are shared across both. *Area* applies only to RSVQA-HR, while *rural/urban* applies only to RSVQA-LR. Generation is limited to 16 new tokens.

The presence prompt is:

<question>

You must respond with exactly ONE word from the possible answers:

yes

no

Respond immediately. Do not think.

The answer is:

The counting prompt is:

<question>

You must respond with exactly ONE with exactly ONE integer.

IMPORTANT OUTPUT RULES:

Respond immediately. Do not think.

The answer is:

The comparison prompt is:

<question>

You must respond with exactly ONE word from the possible answers:

yes

no

Respond immediately. Do not think.

The answer is:

The area prompt is:

<question>

You must respond with a single integer, followed by the unit m²:

Xm²

where X is the area in square meters covered by the feature.

Respond immediately. Do not think.

The answer is:

The rural/urban prompt is:

<question>

You must respond with exactly ONE word from the possible answers:

yes

no

Respond immediately. Do not think.

The answer is:

Across all prompts, <question> is the question as stated in the dataset.

VRSBench (caption) and OSMDA-Captions. As both datasets contain long, descriptive, single-paragraph captions, we limit the maximum number of new tokens to 512 and use the following prompt:

This is a satellite image of an area.

Please provide a single-paragraph caption describing what is going on in the area.

Use a confident, declarative tone.

Include EVERYTHING visible in the image in your caption and define spatial relationships as best as possible.

VRSBench (vqa). In this dataset, many images are miscategorized, and some have open questions (with a single-phrase answer). We thus limit the maximum new tokens to 32 and use the following prompt:

<question>

Answer concisely and only with the information requested.

Do NOT include unnecessary explanations or extra text.

Format numeric answers with units only if explicitly requested.

Answer immediately, do not think.

The answer is:

<question> is the question as phrased in the dataset.

AID, EuroSAT and SkyScript-Bench. As all datasets consist of multiple-choice classification with a single correct answer, we allow up to 16 new tokens and prompt the models with:

You are performing image classification.

Your response must contain a single word: your classification of the image.

You are given a list of classification options.

If your response is NOT contained in the listed options, that is a CRITICAL

MISTAKE.

Here is the list of your classification options, separated by comma (,):

<comma_separated_MC_list>

Respond with ONE word from this list - your chosen classification, exactly as shown above.

The correct option is:

Where <comma_separated_MC_list> is the list of all possible classes for that dataset, separated by commas. For each dataset, it is static across samples.

Million-AID. This dataset also comprises a single-choice classification task, but each label corresponds to a node in a semantic class hierarchy (for example, agriculture land → arable land → dry field). We thus increase the output tokens to 32, and use a customized prompt which aligns the model better with the input format:

You are performing image classification.

Each image belongs to exactly ONE of the following predefined classes.

These classes are already formatted as concatenations of 2 or 3 elements using hyphens ('-').

You must choose exactly ONE class from the list below.

IMPORTANT OUTPUT RULES:

- Use ONLY one of the provided class names
- Do NOT split the class or combine multiple classes
- Do NOT think, add explanations, extra text, or invent new classes

Class list:

<comma_separated_hyphen_fused_hierarchical_classes> Respond with ONE word from this list - your chosen classification, exactly as shown above.

The correct option is:

Here, <comma_separated_hyphen_fused_hierarchical_classes> denotes a comma-separated list of class labels, where each label represents a hierarchical category path encoded by concatenating its levels with hyphens – e.g. agriculture_land-arable_land-dry_field.

XLRS-Bench. The creators of this dataset provide an official captioning prompt [1]. As it generally results in extremely long and detailed captions, we set a liberal limit to new tokens of 1024 and reuse the prompt as provided in their official repository. The VQAs are multiple-choice, but may contain multiple correct labels. However, each question has a custom small set of options. We thus limit the number of new tokens to 4 and prompt only for a list of letters:

<question>

Select one or more of the options below:

<comma_separated_options>

Do not think. You must output ONLY a sequence of one or more letters:

the letters corresponding to all answers which are correct.
The correct answers are:

Where <question> is the question, and <comma_separated_options> is the list of options for the given question as provided in the dataset.